Characterization of the Surface Properties of Commercially Available Dental Implants Using Scanning Electron Microscopy, Focused Ion Beam, and High-Resolution Transmission Electron Microscopy

Tobias Jarmar, PhD;* Anders Palmquist, MSc;† Rickard Brånemark, MD, PhD;‡ Leif Hermansson, PhD;* Håkån Engqvist, PhD;* Peter Thomsen, MD, PhD†

ABSTRACT

Background: Since osseointegration of the respective implant is claimed by all manufacturing companies, it is obvious that not just one specific surface profile including the chemistry controls bone apposition.

Purpose: The purpose was to identify and separate out a particular set of surface features of the implant surfaces that can contribute as factors in the osseointegration process.

Material and Methods: The surface properties of several commercially available dental implants were extensively studied using profilometry, scanning electron microscopy, and transmission electron microscopy. Ultrathin sections prepared with focused ion beam microscopy (FIB) provided microstructural and chemical data which have not previously been communicated. The implants were the Nobel Biocare TiUnite® (Nobel Biocare AB, Göteborg, Sweden), Nobel Biocare Steri-Oss HA-coated (Nobel Biocare AB, Yorba Linda, CA, USA), Astra-Tech OsseoSpeed™ (Astra Tech AB, Mölndal, Sweden), Straumann SLA® (Straumann AG, Waldenburg, Switzerland), and the Brånemark Integration Original Fixture implant (Brånemark Integration, Göteborg, Sweden).

Results: It was found that their surface properties had differences. The surfaces were covered with crystalline TiO_2 (both anatase and rutile), amorphous titanium oxide, phosphorus doped amorphous titanium oxide, fluorine, titanium hydride, and hydroxyapatite, respectively.

Conclusion: This indicates that the provision of osseointegration is not exclusively linked to a particular set of surface features if the implant surface character is a major factor in that process. The studied methodology provides an effective tool to also analyze the interface between implant and surrounding bone. This would be a natural next step in understanding the ultrastructure of the interface between bone and implants.

KEY WORDS: dental implants, FIB, osseointegration, profilometry, SEM, surface morphology, TEM, titanium, ultrastructure

Titanium screws have been the most used dental implant for decades. Ever since the discovery that Ti may integrate in bone tissue,[1] many types of Ti implants have been used for reconstructions and repair of bone. The original implant was structured by a machining process and performs well in the human body. However, the strive for improved results in compromised tissues, a reduction of the initial healing period, and increased competition between manufacturers have driven them to modify the implant surfaces allegedly enhancing osseointegration. In this study, we have analyzed five of

*Department of Engineering Sciences, Uppsala University, Box 534, SE-751 21 Uppsala, Sweden; †Department of Biomaterials, Sahlgrenska Academy, Göteborg University, Box 412, SE-405 30 Göteborg, Sweden; ‡Department of Orthopaedics, Sahlgrenska University Hospital, Göteborg University, SE-413 45 Göteborg, Sweden

Reprint requests: Tobias Jarmar, Doxa AB, Axel Johanssons gata 4-6, SE-754 21 Uppsala, Sweden; e-mail: tobias.jarmar@doxa.se

DOI 10.1111/j.1708-8208.2007.00056.x

the most common dental implants, from a machined Ti screw via sandblasted and etched screws to coated ones.

The outermost surface is naturally the most important feature of the implant with respect to osseointegration; therefore, this study contributes with a visualization and chemical analysis of it. These surface differences have usually been extensively analyzed with respect to clinical performance.[2,3] Interestingly, there are only a few publications addressing the surface structure and elemental composition at high magnification, that is, ultrastructural studies.

One reason for the few reported high-resolution studies is likely that it is very difficult to prepare samples that have good-enough quality to enable ultrastructural characterization, that is, morphology, crystallinity, and elemental distribution, for transmission electron microscopy (TEM). The TEM sample must be prepared carefully to make it very thin (~100 nm or less). The focused ion beam (FIB) microscope is ideal for this purpose. With the FIB, TEM samples can be prepared with submicron site specificity from almost any material. These samples can then be directly transferred to a TEM for high resolution, chemical, and crystallinity analysis.

In this article, five commercially available implants (Nobel Biocare TiUnite®, Nobel Biocare AB, Göteborg, Sweden; Nobel Biocare Steri-Oss® hydroxylapatite (HA) coated, Nobel Biocare, Yorba Linda, CA, USA; Astra Tech OsseoSpeed®, Astra Tech AB, Mölndal, Sweden; Straumann SLA®, Straumann AG, Waldenburg, Switzerland; and the Brånemark Integration Original Fixture Implant, Brånemark Integration, Göteborg, Sweden) were studied. The TiUnite surface is produced by anodic oxidation, which creates its porous surface structure. Anodic oxidation is an electrochemical process where the implant is immersed in an electrolyte while a current is applied which will make the implant the anode in an electric cell; this will oxidize the implant. The electrolyte used and the current applied for the TiUnite are, however, unknown. The OsseoSpeed surface is a fluoride-modified TiO_2 blast surface. The TiO_2 blast surface is made of commercially pure Ti, which is grit blasted with 25 μm TiO_2 particles.[4] The subsequent fluoride modification, which OsseoSpeed undergoes, is a diluted hydrofluoric acid treatment.[4,5] The resulting surface structure of the mentioned treatments gives an isotropic roughness; hence, no preferred direction of the surface irregularities.[5] The name of the Straumann surface, SLA, is an abbreviation for sandblasted, large grit, acid etched. The large grits for the sandblasting are corundum particles in the size range of 0.25 to 0.5 mm.[6–8] The sandblasting is followed by an acid etch in tempered HCl/H_2SO_4.[6,7] These processes leave pits and craters. The pits have an average diameter of 1 μm, and they coalesce to form the larger craters with an average diameter of 10 μm.[8] The Brånemark original implant represents the pure Ti surface and was also included in the study. This screw had been turned, machined, and autoclaved before packaging and is considered to represent a minimally rough Ti surface.[9]

MATERIALS AND METHODS

Five different commercially used Ti implants, shown in Table 1, were purchased and subsequently analyzed with respect to their surface roughness and morphology. The roughness was measured by interference profilometry. The surface morphology was analyzed via scanning electron microscopy (SEM) and TEM from low resolution to very high resolution. Elemental analysis by energy-dispersive X-ray spectroscopy (EDS) and energy-filtered TEM (EFTEM) was conducted in the TEM. X-ray photoelectron spectroscopy (XPS) was used to confirm the fluorine content on the OsseoSpeed surface. The TEM sample preparation was made in an FIB microscope.

Profilometry

The implants were transferred from their storage boxes as delivered to a WYKO NT-2000 (Veeco Instruments, Inc., New York, USA) 3D interference microscope, in order to measure the surface roughness. The results were averaged over two surface scans (119×91 μm) in the thread valley of the implants and presented as the arithmetic mean value S_a with SD. The resolution level of the equipment was in vertical axis 3 nm and in the lateral plane 0.5 μm. The measurements were corrected with regard to the implant cylindrical shape with the software of the microscope. An additional overview scan (605×460 μm) was performed to be able to see the form of the threads and cylindrical center of the implant.

Microscopy

SEM. All samples were taken from their storage boxes as delivered from the supplier. They were handled with tweezers and plastic gloves in a clean room environment. Each implant was subsequently attached with an

TABLE 1 Dental Implants Included in this Study

Implant	Lot Number	Cat Number	Reference	Expiry Date	Analysis
Nobel Biocare TiUnite	341252	62003		2007-05	TEM analysis
	669821		28913	2011-08	Profilometry
Nobel Biocare HA coated	339530	61078		2007-03	TEM analysis
	339530	61078		2007-03	Profilometry
Astra Fixture MT 3.5 OsseoSpeed	28698		24511	2010-06	TEM analysis
	28698		24511	2010-06	Profilometry
	31591		24511	2010-12	XPS analysis
Straumann standard implant SLA	1072		043.132S	2010-06	TEM analysis
	1072		043.132S	2010-06	Profilometry
Brånemark Integration Fixture Original 8.5	02-05-019-01		BI-00006	2007-05	TEM analysis
	02-05-019-01		BI-00006	2007-05	Profilometry

HA = hydroxylapatite; TEM = transmission electron microscopy; XPS = X-ray photoelectron spectroscopy.

adhesive carbon tape as well as an aluminum tape on an SEM sample stub. Hereafter, the samples were inserted in a Leo 1550 (Carl Zeiss, Oberkochen, Germany) FEG–SEM operated at 20 kV. All images were acquired with secondary electron detectors in the magnification range from 50 to 150,000 times of which only some selected are shown in this article.

FIB. Prior to insertion in the dual-beam FIB microscope, some samples were sputter coated with a thin film of Au/Pd to protect the implant surface during the initial alignments of the FIB. On samples where a thin oxide was studied, the surface was protected with an electron-beam-deposited Pt layer inside the FIB. The Dualbeam FEI strata 235 FIB (FEI Company, Eindhoven, the Netherlands) has one ion gun column and one electron gun column separated by an angle of 52°. The ion column utilizes a Ga^+ source where the ions are accelerated at 30 kV and with different ion currents used for cutting or imaging of the sample structure. It is also used for depositing a protective Pt layer over the area intended for TEM sample preparation. The electron gun operated at 5 to 10 kV was used for nondestructive high-resolution imaging as well as preprotection layer (Pt) deposition. With the FIB, thin (~100 nm) TEM lamellae can be cut with µm site-specific precision and transferred to a TEM grid in several ways.[10–13]

TEM. For high-resolution imaging, diffraction, and elemental analysis transmission electron microscopes were employed. A JEOL 2000FX (JEOL Ltd., Tokyo, Japan) with a LaB_6 filament operated at 200 kV was used for bright field (BF) imaging as well as selected area diffraction (SAD). Scanning TEM (STEM) combined with EDS, EFTEM, as well as high-resolution TEM (HRTEM) was performed in the FEI Tecnai F30 ST equipped with a Gatan Imaging Filter (Gatan, Inc., California, USA) and was operated at 300 kV. The e-beam spot size was about 1 nm during STEM/EDS acquisitions. The low-magnification BF imaging was made to study the implant surface morphology and was combined with SAD to verify the different crystalline phases present at the surface of some of the implants. The chemistry of the surfaces/coatings was characterized via EDS in STEM mode as well as by EFTEM. Structure determination via HRTEM (lattice imaging) was also conducted.

XPS. The XPS is a highly surface-sensitive method that was used for analyzing the OsseoSpeed surface in the search for fluorine. Only the outermost 10 to 50 Å of the original surface was analyzed in one spectrum. For analytical information at greater depths, depths profiling with Ar ions can be used. This measurement was conducted on a Physical Electronics Quantum 2000 (Physical Electronics, Inc., Minnesota, USA) using Al K_α (1486.6 eV) radiation.

RESULTS

TiUnite

The roughness value was measured to $S_a = 1.55 \pm 0.01$ µm according to interference profilometry. The

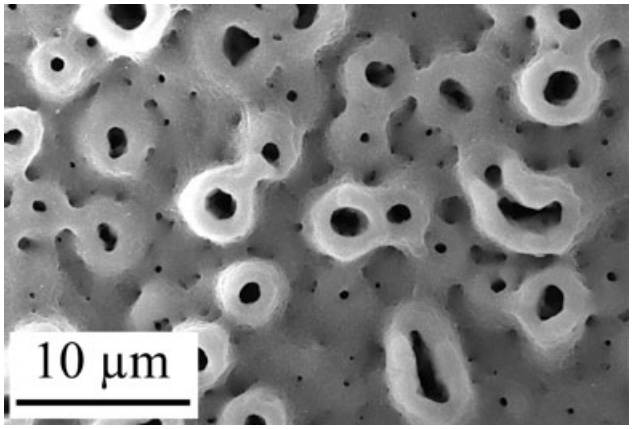

Figure 1 Scanning electron micrograph of the TiUnite implant with its characteristic pores that stand up from the surface.

SEM images show that the TiUnite implant has a rough surface with many pores that stand up like volcanoes from the implant surface (Figure 1). The size of these pores varies between 0.06 and 12 µm. The pore depth is, however, unknown. The sample was therefore prepared from a site between micropores (Figure 2) on the first thread from apex with the ex situ lift-out technique and placed on a holey carbon TEM grid, which was transferred to the TEM for further analysis. By these measurements, the coating was found to be about 2 µm thick on the first thread. The whole coating is visible in a BFTEM image (Figure 3A). At the bottom of the image, the pure Ti is present, going upward to the interface between Ti and the dense amorphous titanium oxide. There is a porous layer consisting of titanium oxide. Further, there are some large pores present in the denser amorphous titanium oxide. Large crystalline clusters are embedded in the surrounding amorphous oxide matrix. At the implant surface, there is only amorphous titanium oxide, but one should bear in mind that the sample is only a few microns wide so there might be areas where the surface looks different. According to SAD (see Figure 3B), the crystalline grains present in the amorphous titanium oxide matrix are anatase TiO_2 although a few spots could originate from the thermodynamically more stable rutile TiO_2. From the center of the figure, the (101) ring appears strongest as expected for randomly oriented oxide grains. The other indexed spots are originating from (004) and (200) anatase TiO_2. HRTEM analysis of a crystalline grain (lattice imaging of (101) with $d = 3.5$ Å) (see Figure 3C) confirms the anatase phase and also shows the adjacent amorphous oxide. The elemental distribution is shown from inside the Ti up to the implant surface (Figure 4A). The Ti signal dominates in the Ti implant, but there was also O present from the native oxide formed on the Ti of the TEM sample. In the porous interface, Ti and O peaks were dominant, and according to the high-resolution study (see Figure 4B), there was no P present in this layer.

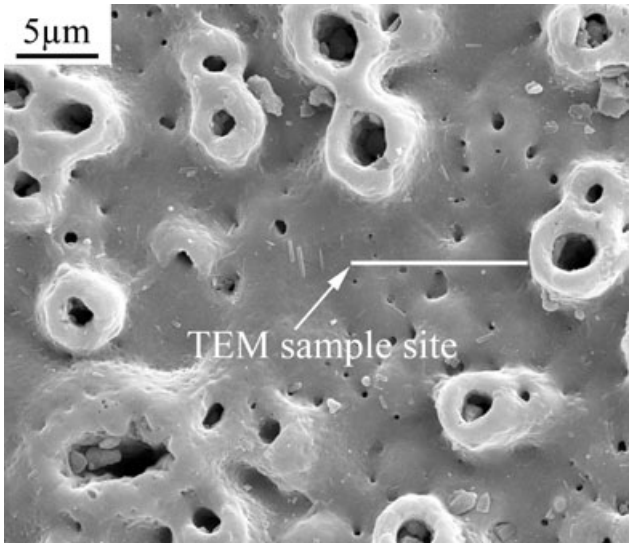

Figure 2 Scanning electron microscopy image of the area where the transmission electron microscopy sample was made.

HA Coated

The surface roughness of this implant was $S_a = 3.29 \pm 1.15$ µm. However, SEM analysis in a micron scale shows that there are flat areas of the HA coating (Figure 5). In some areas, it was evident that the HA coating had cracked. However, it did not flake off (see Figure 5). The TEM sample was lifted out in situ in the FIB from the first thread from apex; unfortunately, the sample did not reach all the way down to the Ti part of the implant. Therefore, the total coating thickness is still unknown. From the TEM analysis, it was found that the top 1 to 2 µm of the HA layer is amorphous while the rest is crystalline (Figure 6). According to both SAD (not shown) and HRTEM (Figure 7), it fits well with the HA JCPDS reference file,[14] which means it is the hexagonal packed HA phase with lattice parameters $a = 9.42$ Å and $c = 6.88$ Å. The HA(101) with a lattice spacing of 5.3 Å is imaged in Figure 7. The bubbles present in the background were created during electron beam irradiation. EDS was also performed for quantification of the Ca/P ratio. However, it was found that the sample was

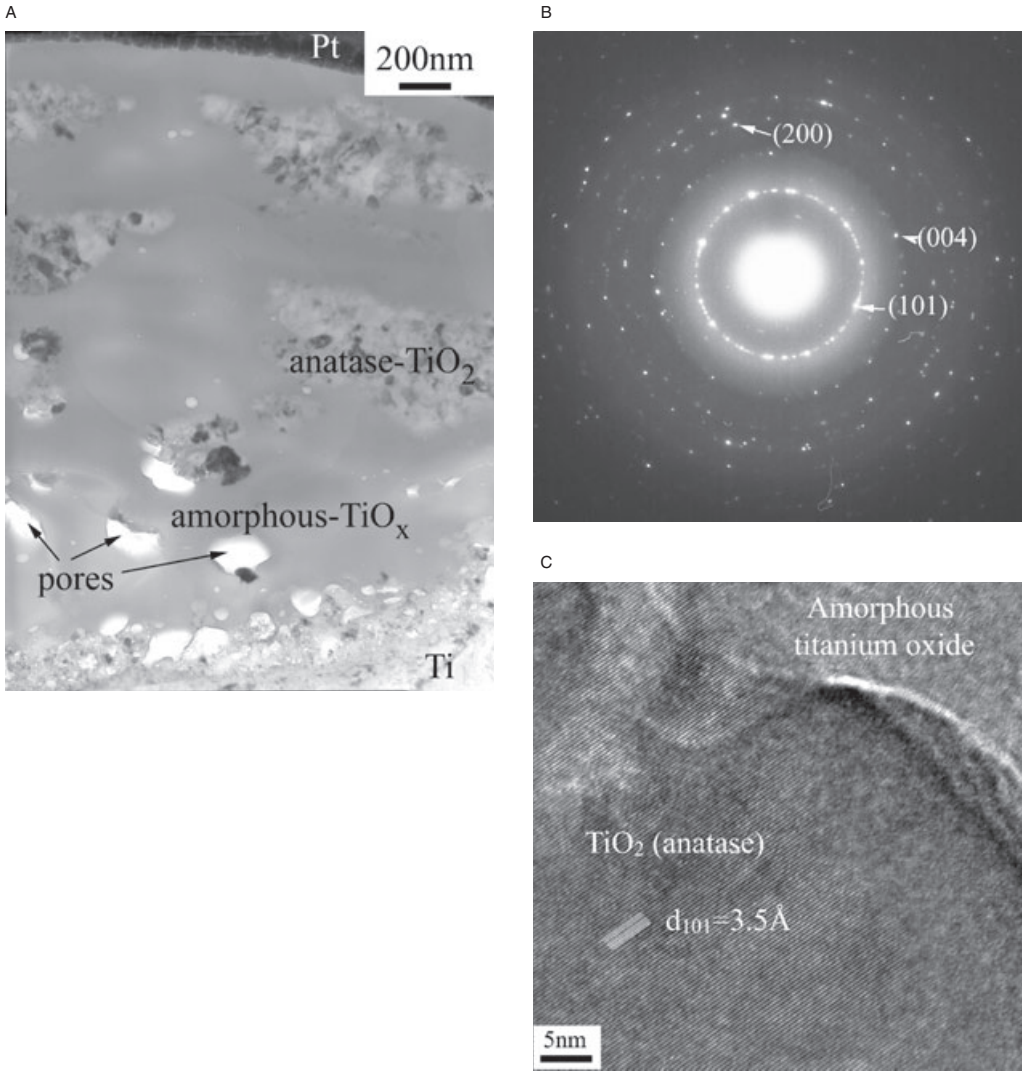

Figure 3 *A*, A transmission electron micrograph of the TiUnite coating down to the Ti substrate showing the morphology as well as the crystalline phases present in the layer. *B*, Selected area diffraction pattern acquired with a 2 μm selected area aperture that allowed the whole coating to be analyzed in one pattern. The diffuse ring likely corresponds to the amorphous titanium oxide, and the three indexed diffraction spots are originating from the anatase TiO_2 phase. *C*, high-resolution transmission electron microscopy showing an anatase grain adjacent to the amorphous oxide. The lattice spacing imaged is the (101) of anatase TiO_2.

extremely sensitive to electron beam damage, which led to large variations in elemental composition between different EDS measurements.

OsseoSpeed

From our analysis, we have found that the OsseoSpeed implant had a macroscopically rough and microscopically island-like surface structure as shown in the SEM image (Figure 8). As it was etched in diluted HF during processing, it is likely that the islands consist of thick titanium oxide, whereas the lower surfaces are where the oxide has been etched away. To study the morphological difference between an island and the lower surface, two TEM specimens were prepared in the FIB. The first sample studied was that of an island, which is presented in Figure 9. The island consisted of a porous mixture of anatase and rutile TiO_2, and it varied in thickness between 0.5 and 1 μm in the specimen made. The HF was supposed to leave remains of F on top of the oxide. The fluorine was not detected by EDS in the TEM sample. However, it was found by analyzing the implant surface by XPS (Figure 10). Another TEM sample prepared over an area where no island was visible shows (Figure 11, A and B) that the oxide layer can be very thin down to 10 nm and of amorphous structure (see Figure 11B).

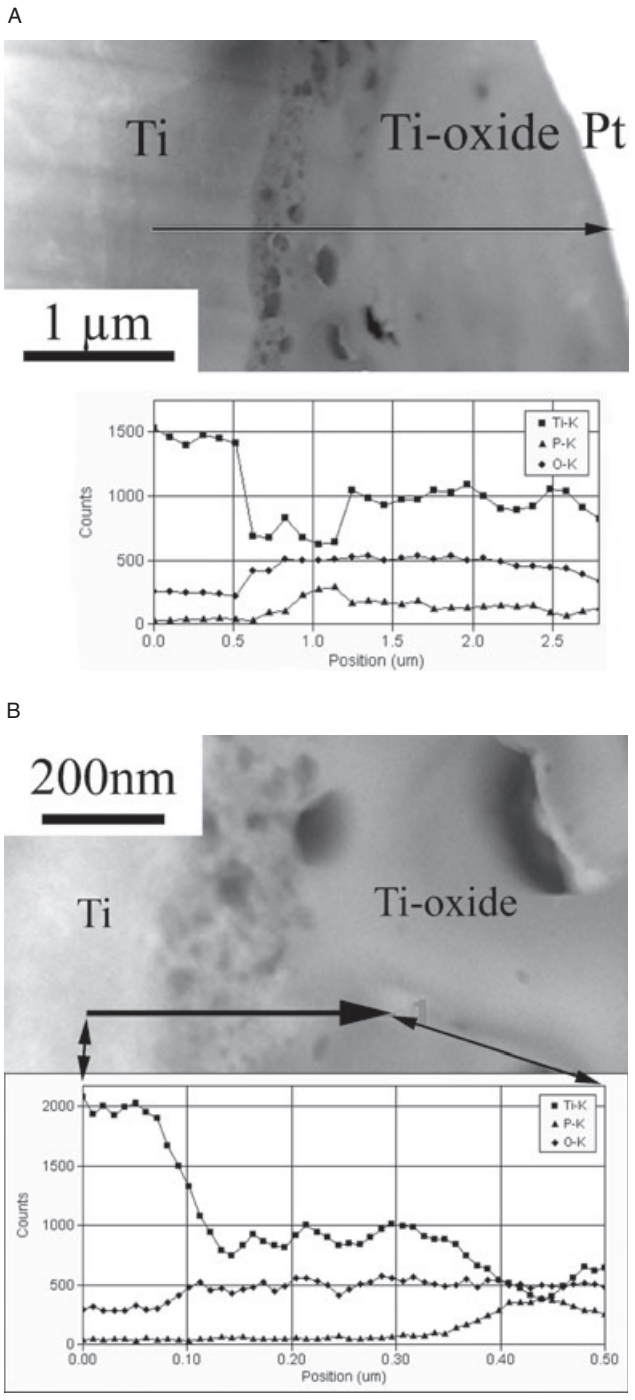

Figure 4 *A*, A scanning transmission electron microscopy (STEM) image showing the sample from Ti substrate to the implant surface. The arrowed line marks where the energy-dispersive X-ray spectroscopy (EDS) line scan was acquired. The underlying graph shows the integrated intensities from Ti, O, and P spectra along the line. *B*, The interface between the amorphous oxide and the Ti consists of a porous titanium oxide without any P according to the STEM/EDS analysis shown in the figure.

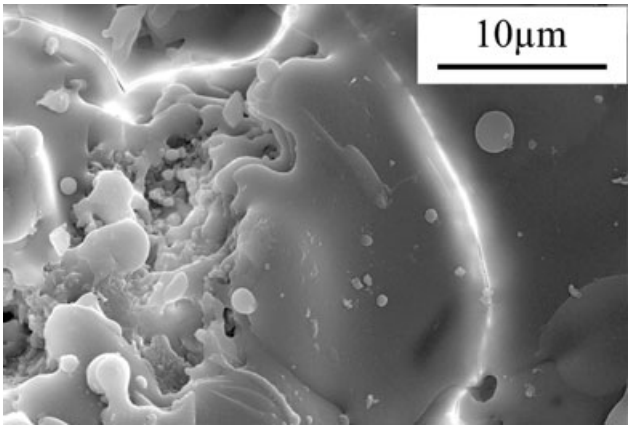

Figure 5 A scanning electron microscopy image showing the surface morphology of, and the cracks in, the hydroxylapatite coating.

SLA

This implant had one of the roughest surfaces according to the profilometry measurement in Table 2. The roughness value (S_a) was measured to be 1.98 ± 0.08 µm, which is somewhat smaller than the referred values. The large roughness can also be seen in the SEM image (Figure 12) where the surface was characterized by dimples and very sharp edges. The morphology of the Straumann SLA surface can be studied from a cross-sectional TEM sample (Figure 13). A high density of dislocations was found in the surface region of the implant. These probably originate from sandblasting during manufacturing. In our SAD and HRTEM investigations, the titanium hydride was not identified. In addition, no hexagonal α-Ti phase or tetragonal anatase or rutile TiO_2 phases were found.[15–17]

Brånemark

The original dental implant surface is the as-machined surface. This implant had a roughness value

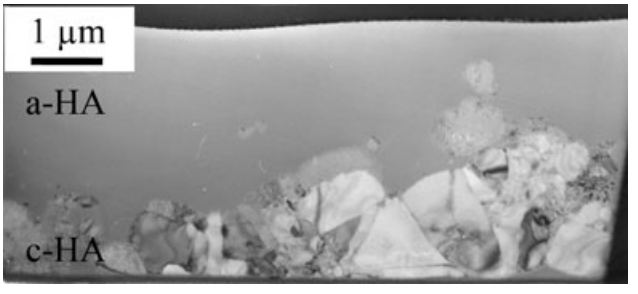

Figure 6 A bright field transmission electron microscopy image showing the amorphous and crystalline hydroxylapatite coating on the Steri-Oss implant.

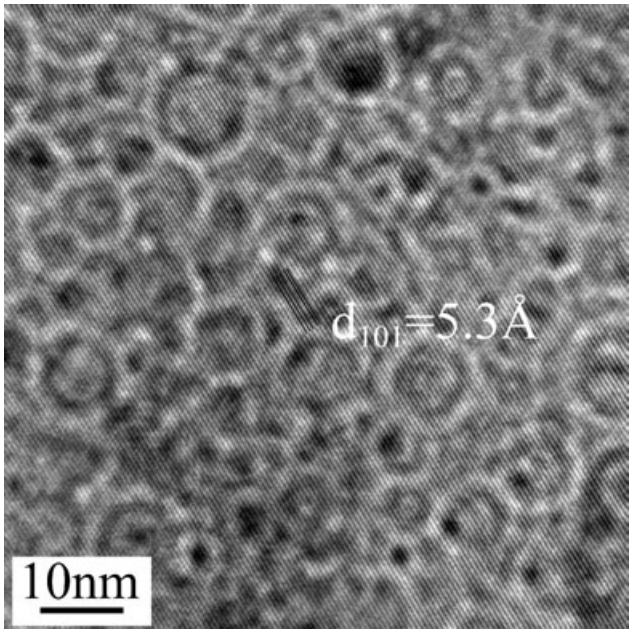

Figure 7 A high-resolution micrograph of the crystalline hydroxylapatite (HA). The indexed plane is the HA(101) with a lattice spacing of 5.3 Å. The ring pattern in the background shows the continuous damage of the sample by the electron beam.

$S_a = 1.53 \pm 0.05$ µm, however very anisotropic which was reflected in the SEM analysis (Figure 14). The topography is mainly created during the machining of the implant, which leaves scratches on the surface where the bottom of a thread is rougher than the top surfaces. From the TEM analysis (Figure 15), the smooth surface

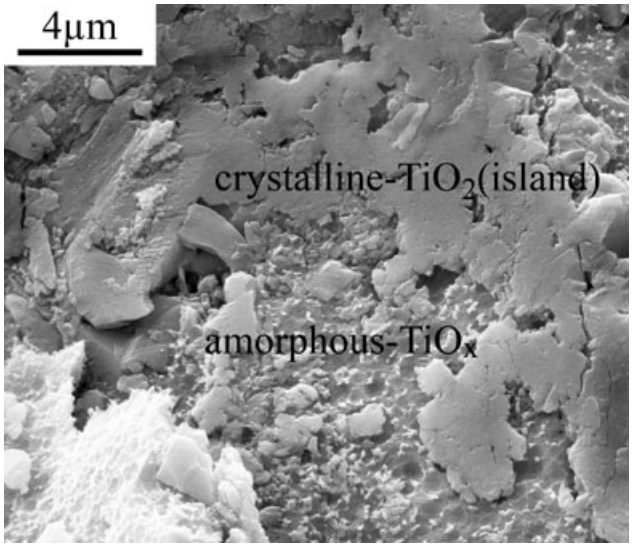

Figure 8 The OsseoSpeed surface is characterized by its roughness and islands according to scanning electron microscopy analysis.

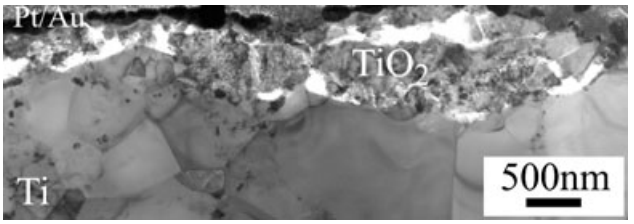

Figure 9 A bright field transmission electron microscopy image of an island from the OsseoSpeed surface. It is a mixture of anatase and rutile TiO_2 without fluorine according to energy-dispersive X-ray spectroscopy measurements in the transmission electron microscopy.

is shown with the underlying polycrystalline Ti. The titanium oxide was measured to be 10 nm thick and crystalline of unknown phase (see Figure 15). The contrast difference between the ion-beam- and the electron-beam-deposited Pt layers is pronounced (Figure 16). The Pt and Ti were found to be easily identifiable, whereas the interface between them, that is, the Ti surface, was not. To confirm the oxygen content of the surface, energy-filtered images were acquired in the TEM.[12] High-resolution TEM showed that the titanium oxide on the surface was rutile TiO_2.[12]

DISCUSSION

TiUnite

The typical roughness value from references is $R_a = 1.2$ µm[18,19]; however, Sammons and colleagues[20] reported a roughness value of $R_a = 0.76 \pm 0.14$ µm. The value determined in the present study by interference profilometry gave $S_a = 1.55$ µm. Although this value is higher than previously reported, it is possible that it is related to the employed analytical technique. Further,

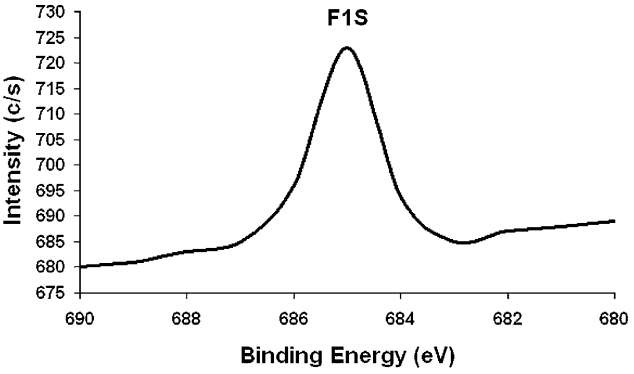

Figure 10 X-ray photoelectron spectroscopy shows that fluorine is present on the implant surface; however, its binding state is unknown.

TABLE 2 A Comparison of the Dental Implants Surface Properties

Implant	Surface Modification	$S_a \pm SD$ (μm)	Surface Layer Thickness (μm)	Surface Chemistry	Comments
TiUnite	Anodic oxidation	1.55 ± 0.01	2	Amorphous $TiO_x + TiO_2$ (anatase) + phosphorus	
HA	Plasma-sprayed hydroxyapatite	3.29 ± 1.15	>5	Amorphous + crystalline HA	TEM sample not deep enough to measure coating thickness
OsseoSpeed	Grit blasted + diluted HF etch	1.82 ± 0.12	0.5–1	TiO_2 (anatase + rutile)	Upper surface (island)
			0.01	Amorphous	Lower surface
SLA	Grit blasted + acid etched	1.98 ± 0.08	—	TiH_x[24]	Not possible to find surface structure
Brånemark Integration	Turned, machined	1.53 ± 0.05	0.01	TiO_2 (rutile)	Surface roughness highly anisotropic

HA = hydroxyl apatite.

Figure 11 *A*, A bright field transmission electron microscopy micrograph showing the morphology of the Ti surface where no island was present. *B*, The high-resolution analysis identifies the surface oxide as being amorphous and about 10 nm thick. The lattice plane imaged is the Ti (100) with 2.5 Å spacing (OsseoSpeed).

the roughness might vary at different areas of the implant. Different measuring techniques may give different roughness values.[21]

The SEM-measured pore size distribution, 0.06 to 12 μm, is in accordance with previous data[22] where micropores (1 to 7 μm) and nanopores (<1 μm) were found. This porosity increases the difficulty of making good TEM samples, at least over a pore. One way could be to fill up the pore with either some polymer resin or by electron-assisted in situ deposition of Pt using the FIB. The TEM sample was in this case prepared over a relative pore-free area.

The TiUnite surface oxide coating is the thickest in this study with a thickness of 2 μm. According to X-ray

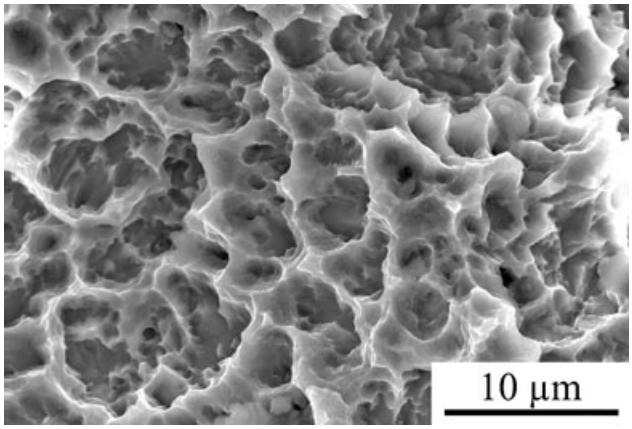

Figure 12 The sharp-edged and dimple-rich Straumann SLA surface imaged by scanning electron microscopy.

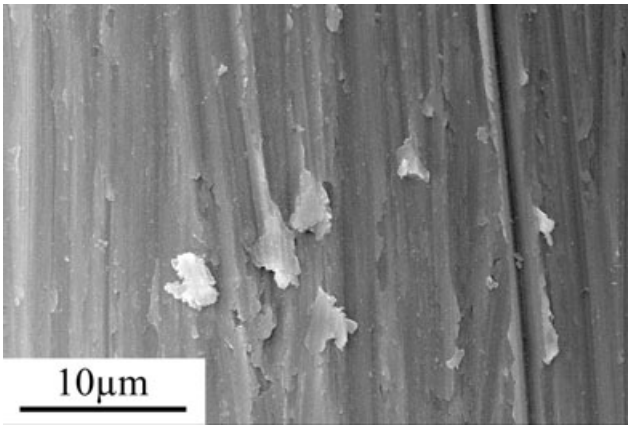

Figure 14 The machined surface of the Brånemark Integration 8.5 implant viewed by scanning electron microscopy.

diffraction measurements made by Hall and Lausmaa,[19] the coating consists of both rutile and anatase TiO_2; their fractions are, however, unknown. The electron diffraction and HRTEM analysis showed that only anatase TiO_2 was present in the limited volume that was analyzed. A substantial amount of phosphorus was found in the coating according to EDS measurements in the TEM. It was also demonstrated by point EDS analysis that P is present both in the crystalline and the amorphous oxide. The P distribution in the coating from the Ti substrate up to the surface seems to be rather constant except in the porous interface between substrate and coating where it is low. Phosphorus appeared in the amorphous oxide and had a fairly constant concentration throughout the coating all the way up to the surface.

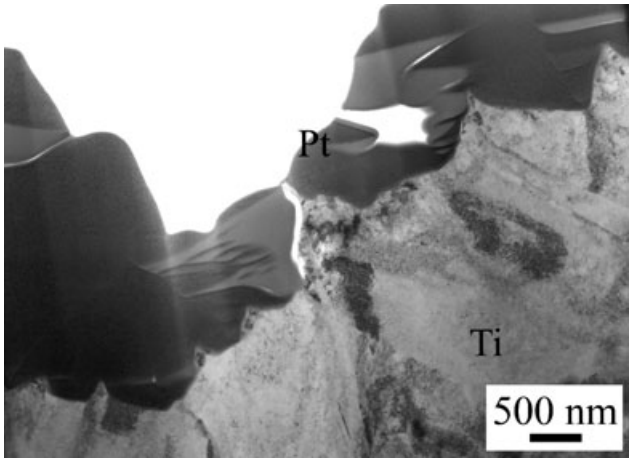

Figure 13 A transmission electron microscopy cross-sectional bright field image of the SLA-treated Ti implant made by Straumann.

According to Hall and Lausmaa,[19] there is 5% phosphorus in the surface layer in the form of phosphates.

HA Coated

This implant is very rough, and it is actually the roughest in this study. The surface is, however, locally very flat. The coating appears to contain a fairly large density of cracks. It is unknown how deep these cracks are, but there is no tendency of flaking. The surface is composed of amorphous HA whereas the rest of the analyzed sample is crystalline. The amorphous HA might dissolve

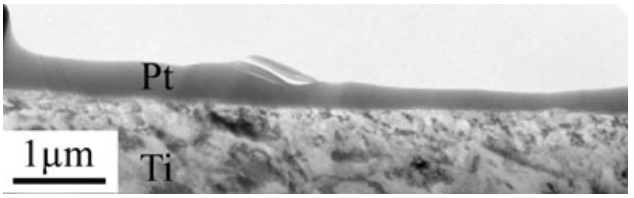

Figure 15 The smooth surface of the reference sample showed in an cross-sectional transmission electron microscopy image.

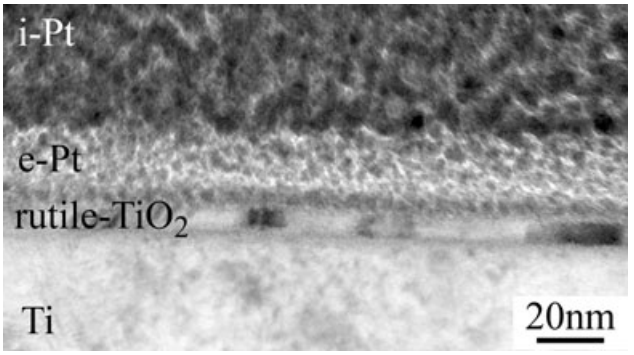

Figure 16 At higher magnification, the crystalline titanium oxide thickness was measured to 10 nm.

when it is implanted.[23] Studies have focused on the role of HA crystallinity for bone formation and bone bonding, but no consensus as to the optimal features has been reached so far. In contrast to relatively thick HA coatings bearing a risk for delamination and fragmentation, usually prepared by plasma-spraying technique, recent experimental in vivo studies have utilized micron- and submicron-thick calcium phosphates with very good results.[24–26] Hitherto, the manufacturers of oral implants have not reported any clinical data using such thin calcium phosphate coatings.

OsseoSpeed

The surface roughness is created during the grit-blasting process, while the diluted hydrofluoric acid reduces the high peaks slightly. Studies report $S_a = 0.91 \pm 0.14$ μm for OsseoSpeed compared to $S_a = 1.12 \pm 0.24$ μm for TiO_2 blast.[4,5] These values deviate from our results where the S_a value was measured to be 1.82 ± 0.12 μm. The hydrofluoric acid treatment does not only slightly change the microstructure, but also changes the surface chemistry. According to Masaki and colleagues,[4] the atomic weight percentage of fluoride on the oxide surface is 1%. Further, according to Ellingsen and colleagues,[5,27] the surface fluoride incorporated in the oxide will serve as a precipitation site for calcium and phosphorus and also allows covalent bonding to the phosphate to create fluoridated hydroxyapatite and fluorapatite. From the TEM measurements, it was found that the TiO_2 island consisted of both rutile and anatase. The thickness varied in the interval 0.5 to 1 μm. Whether a diluted hydrofluoric acid treatment changes the titanium oxide layer is uncertain, but according to Eriksson and colleagues[28] who etched polished Ti, native and annealed, in 10% HF for 3 minutes a reduction of the oxide thickness was detected, from 36 to 29 nm for the annealed specimens. This indicates that the F-containing layer was very thin and might be removed during deposition of the protective Pt layer, or that the F content was very low, below a few atomic percent. Fluorine is known to be a volatile element that might easily disappear during the preparation and e-beam irradiation.

SLA

Different roughness values have been reported using different measuring methods. Buser and colleagues[29] found $R_a = 3.1$ μm on a solid screw-formed implant, and Boyan and colleagues[8] found a roughness of $R_a = 3.68$ μm when measuring on Ti disks prepared as mentioned. Wieland and colleagues[30] found a roughness $R_a = 4.33 \pm 0.27$ μm for the same surface treatment. Our value measured in the present investigation was lower with $S_a = 1.98 \pm 0.08$ μm. From SEM investigations, it appears that it actually has two levels of roughness, one that is macroscopic and one microscopic. This combined roughness makes the FIB preparation difficult. The Pt layer was uneven in thickness, and therefore, the high peaks were preferentially milled, resulting in difficulties to produce a thin TEM sample. The TEM results showed no expected surface oxide, but a defect dense surface of unknown composition. From a thorough TEM investigation made by Conforto and colleagues[31] on the SLA surface, it was shown that the top layer of the implant consisted of $TiH_{1.971}$. We could not confirm this phase even after thorough electron diffraction studies. Others have found that the surface is composed of TiO_2 using XPS analysis.[7] Furthermore, the oxide layer was measured to be 4.5 to 5.5 nm and composed mainly of TiO_2 but also of some TiO and Ti_2O_3 according to Buser and colleagues.[29] Thermal desorption spectroscopy shows, however, large amounts of hydrogen in the subsurface layer for the SLA surface compared to a polished surface.[6]

Brånemark

According to Wennerberg,[32] the surface roughness of the as-machined Ti surface is $S_a = 0.71$ μm. Hall and Lausmaa[19] measured the roughness value for the Nobel Biocare Brånemark MKIII as-machined implant, $R_a = 0.81 \pm 0.08$ μm. The value found in the present investigation was higher than these measurements, but there should be a difference at different parts of the surface. The combination of EFTEM and HRTEM of the oxygen-containing crystalline layer where an interplanar spacing of 2.06 Å was measured was found to correspond closely to the rutile TiO_2. This investigation was reported in detail by Jarmar and colleagues.[12]

COMPARISON

A comparison of these implants is not clear-cut because the surfaces display large ultrastructural differences. In Table 2, some of the key findings have been summarized. The surface modification process is not easily accessible, while they are company secrets. The thickness of the surface layer is straightforward to measure, but it is

probably not constant over the surface. That is also the case with the surface chemistry. From a biological/chemical point of view, these manufacturers probably have different theories regarding osseointegration enhancement, while the topography, surface chemistry, and crystallinity are very different.

CONCLUSIONS AND OUTLOOK

The present study of different commercially available dental implants gives new information regarding their surface properties. The thorough evaluation comprises examination of the surface profile, phases of the surface region, micro- and nanostructure, and the interface to the substrate metal. It is evident that all manufacturers have found totally different ways of modifying the surface in order to enhance the osseointegration. It would be natural to analyze the same type of implants after they have been retrieved from an animal or a human. In essentially the same manner, we would be able to extract samples of intact interfaces between material and tissue for further TEM studies. That could give an indication of how well these implants osseointegrate and how the implant surface should be modified.

ACKNOWLEDGMENTS

Support from the VINNOVA VinnVäxt Program Biomedical Development in Western Sweden, the Swedish Research Council (grant K2006-73X-09495-16-3), the Göran Gustafsson Foundation, Doxa AB, and Integrum AB is gratefully acknowledged.

REFERENCES

1. Branemark P-I, Hansson BO, Adell R, et al. Osseointegrated implants in the treatment of the edentulous jaw. Experience from a 10-year period. Scand J Plast Reconstr Surg 1977; 16:1–132.
2. Esposito M. Titanium for dental applications (I). In: Brunette DM, Tengvall P, Textor M, Thomsen P, eds. Titanium in medicine. New York, NY: Springer Verlag, 2001:827–873.
3. Buser D. Titanium for dental applications (II): implants with roughened surfaces. In: Brunette DM, Tengvall P, Textor M, Thomsen P, eds. Titanium in medicine. New York, NY: Springer Verlag, 2001:875–888.
4. Masaki C, Schneider GB, Zaharias R, Seabold D, Stanford C. Effects of implant surface microtopography on osteoblast gene expression. Clin Oral Implants Res 2005; 16:650–656.
5. Ellingsen JE, Johansson CB, Wennerberg A, Holmén A. Improved retention and bone-to-implant contact with fluoride-modified titanium implants. Int J Oral Maxillofac Implants 2004; 19:659–666.
6. Taborelli M, Jobin M, François P, et al. Influence of surface treatments developed for oral implants on the physical and biological properties of titanium; I: surface characterization. Clin Oral Implants Res 1997; 8:208–216.
7. Information by Straumann. The Straumann SLA® Implant Surface: clinically proven reduced healing time. http://www.straumann.com. (Accessed October 20, 2006)
8. Boyan BD, Batzer R, Kieswetter K, et al. Titanium surface roughness alters responsiveness of MG63 osteoblast-like cells to 1α,25-$(OH)_2D_3$. J Biomed Mater Res 1998; 39:77–85.
9. Albrektsson T, Wennerberg A. Oral implant surfaces: part 1 – review focusing on topographic and chemical properties of different surfaces and in vivo responses to them. Int J Prosthodont 2004; 17:536–543.
10. Langford RM, Petford-Long AK. Preparation of transmission electron microscopy cross-section specimens using focused ion beam milling. J Vac Sci Technol A 2001; 19:2186–2193.
11. Bicais-Lepinay N, Andre F, Pantel R, Jullian S, Margain A, Kwakman LFTz. Lift-out techniques coupled with advanced TEM characterization methods for electrical failure analysis. Microel Rel 2002; 42:1747–1752.
12. Jarmar T, Palmquist A, Brånemark R, Hermansson L, Engqvist H, Thomsen P. Technique for preparation and characterization in cross-section of oral titanium implant surfaces using focused ion beam and transmission electron microscopy. J Biomed Mater Res A. (Accepted for publication)
13. Engqvist H, Botton GA, Couillard M, et al. A novel tool for high-resolution transmission electron microscopy of intact interfaces between bone and metallic implants. J Biomed Mater Res 2006; 77:20–24.
14. JCPDS–International Center for Diffraction Data. PDF file no. 09-0432 (Hydroxylapatite), 2005.
15. JCPDS–International Center for Diffraction Data. PDF file no. 044-1294 (Titanium), 2005.
16. JCPDS–International Center for Diffraction Data. PDF file no. 021–1272 (TiO_2, anatase), 2005.
17. JCPDS–International Center for Diffraction Data. PDF file no. 021-1276 (TiO_2, rutile), 2005.
18. Zechner W, Tangl S, Fürst G, et al. Osseous healing characteristics of three different implant types, a histologic and histomorphometric study in mini-pigs. Clin Oral Implants Res 2003; 14:150–157.
19. Hall J, Lausmaa J. Properties of a new porous oxide surface on titanium implants. Appl Osseoint Res 2000; 1:5–8.
20. Sammons RL, Lumbikanonda N, Cantzler P. Osteoblast interactions with a FRIADENT experimental surface and other microstructured dental implant surfaces. In: 10th

International FRIADENT Symposium Mannheim/ Heidelberg, 2003. http://www.friadent.de. (Accessed December 8, 2005)

21. Wennerberg A. On surface roughness and implant incorporation. PhD thesis, Göteborg University, Göteborg, Sweden, 1996.
22. Schüpbach P, Glauser R, Rocci A, et al. The human bone-oxidized titanium implant interface: a light microscopic, scanning electron microscopic, back-scatter scanning electron microscopic, and energy-dispersive X-ray study of clinically retrieved dental implants. Clin Implant Dent Relat Res 2005; 7:36–43.
23. Lo WJ, Grant DM, Ball MD, et al. Physical, chemical, and biological characterization of pulsed laser deposited and plasma sputtered hydroxyapatite thin films on titanium alloy. J Biomed Mat 2000; 50:536–545.
24. Mohammadi S, Esposito M, Hall J, Emanuelsson L, Krozer A, Thomsen P. Short-term bone response to titanium implants coated with thin radiofrequent magnetron sputtered hydroxyapatite in rabbits. Clin Implant Dent Relat Res 2003; 5:241–253.
25. Mohammadi S, Esposito M, Hall J, Emanuelsson L, Krozer A, Thomsen P. Long-term bone response to titanium implants coated with thin radiofrequent magnetron sputtered hydroxyapatite in rabbits. Int J Oral Maxillofac Implants 2004; 19:498–509.
26. Oh S, Tobin E, Yang Y, Carnes DL, Jr, Ong JL. In vivo evaluation of hydroxyapatite coatings of different crystallinities. Int J Oral Maxillofac Implants 2005; 20:726–731.
27. Ellingsen JE. On the properties of surface-modified titanium. I: Bone engineering. Toronto, Canada: Em Squared, Inc. 2002; 183–189.
28. Eriksson C, Lausmaa J, Nygren H. Interaction between human whole blood and modified TiO_2-surfaces: influence of surface topography and oxide thickness on leukocyte adhesion and activation. Biomaterials 2001; 22:1987–1996.
29. Buser D, Nydegger T, Oxland T, et al. Interface shear strength of titanium implants with a sandblasted and acid-etched surface: a biomechanical study in the maxilla of miniature pigs. J Biomed Mater Res 1999; 45:75–83.
30. Wieland M, Textor M, Chehroudi B, Brunette DM. Synergistic interaction of topographic features in the production of bone-like nodules on Ti surfaces by rat osteoblasts. Biomaterials 2005; 26:1119–1130.
31. Conforto E, Caillard D, Aronsson B-O, Descouts P. Crystallographic properties and mechanical behavior of titanium hydride layers grown on titanium implants. Phil Mag 2004; 84:631.
32. Wennerberg A. The importance of surface roughness for implant incorporation. Int J Tools Manufact 1998; 38:657–662.